Proceedings of the ASME 2018
Dynamic Systems and Control Conference
DSCC2018
September 30-October 3, 2018, Atlanta, Georgia, USA

DSCC2018-9179

ERGODIC EXPLORATION FOR ADAPTIVE SAMPLING OF WATER COLUMNS USING GLIDING ROBOTIC FISH *

Osama Ennasr†
Smart Microsystems Lab
Department of Electrical and Computer Engineering
Michigan State University
East Lansing, MI 48823, USA
ennasros@msu.edu

Giorgos Mamakoukas
Neuroscience and Robotics Lab
Department of Mechanical Engineering
Northwestern University
Evanston, IL 60208, USA
giorgosmamakoukas@u.northwestern.edu

Todd Murphey
Neuroscience and Robotics Lab
Department of Mechanical Engineering
Northwestern University
Evanston, IL 60208, USA
t-murphey@northwestern.edu

Xiaobo Tan
Smart Microsystems Lab
Department of Electrical and Computer Engineering
Michigan State University
East Lansing, MI 48823, USA
xbtan@egr.msu.edu

ABSTRACT

In recent years, gliding robotic fish have emerged as promising mobile platforms for underwater sensing and monitoring due to their notable energy efficiency and maneuverability. For sensing of aquatic environments, it is important to use efficient sampling strategies that incorporate previously observed data in deciding where to sample next so that the gained information is maximized. In this paper, we present an adaptive sampling strategy for mapping a scalar field in an underwater environment using a gliding robotic fish. An ergodic exploration framework is employed to compute optimal exploration trajectories. To effectively deal with the challenging complexity of finding optimum three-dimensional trajectories that are feasible for the gliding robotic fish, we propose a novel strategy that combines a unicycle model-based 2D trajectory optimization with spiral-enabled water column sampling. Gaussian process (GP) regression is used to infer the field values at unsampled locations, and to update a map of expected information density (EID) in the environment. The outputs of GP regression are then fed back to the ergodic exploration engine for trajectory optimization. We validate the proposed approach with simulation results and compare its performance with a uniform sampling grid.

Introduction

Monitoring and understanding aquatic environments is paramount for sustaining water resources and ensuring the longevity of aquatic ecosystems. For that reason, autonomous underwater robots are increasingly drawing attention in aquatic sensing, with applications ranging from marine sciences and tracking oil spills, to monitoring harmful algal blooms and tracking fish movement [1, 2]. Given the ever-changing and unpredictable nature of the environments in which they operate, robots employed for underwater missions need to be both highly energy-efficient and maneuverable [3].

Gliding robotic fish are a recent development in underwater robotic sensing [4], combining the desirable features of both un-

*This work was supported by the National Science Foundation (IIS 1319602, ECCS 1446793, IIS 1715714)

†Address all correspondence to this author.

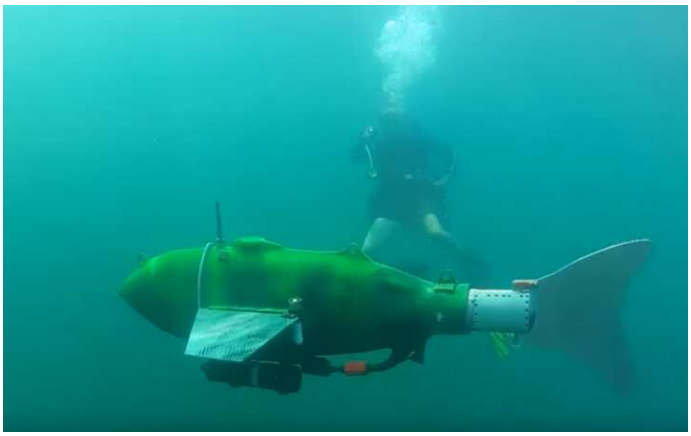

FIGURE 1. The gliding robotic fish "Grace 2.0" during tests in Higgins Lake, Michigan.

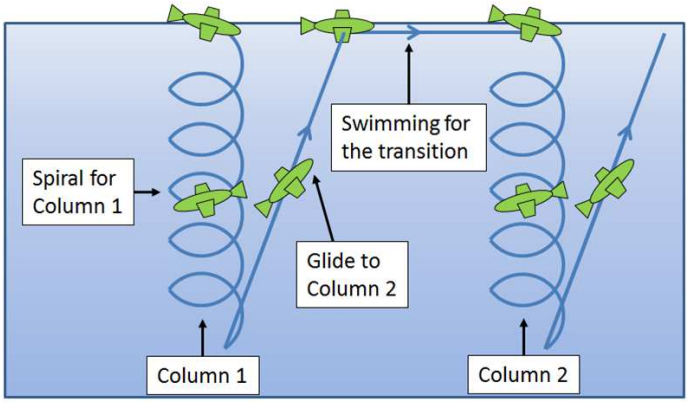

FIGURE 2. Schematic of the autonomous water-column-based sampling scheme using the three operational modes of the gliding robotic fish.

derwater gliders and robotic fish, which are well known for their respective energy efficiency [5–7] and maneuverability [8–10]. These traits allow a gliding robotic fish to realize its locomotion through buoyancy-driven gliding, along with adjustment of its center of gravity to change its pitch. These robots are equipped with actively controlled fins that provide high maneuverability and additional propulsion during locomotion if needed. Figure 1 shows an example of a gliding robotic fish developed by the Smart Microsystems Lab at Michigan State University.

The gliding robotic fish has three main modes of operation. Two of them, gliding and spiraling, are energy-efficient, where most energy is spent when the robot changes its buoyancy and center of gravity. During gliding, the robot either pitches down while being negatively buoyant in order to descend, or pitches up while being positively buoyant to ascend. Spiraling is achieved in a manner similar to gliding, with the tail deflected at a non-zero angle. During a steady-state spiraling operation, the yaw angle changes at a constant rate, while the roll angle and the pitch angles remain constant. It has been shown that the gliding robotic fish can achieve a steady spiraling motion when all three controls (i.e., net buoyancy, center of gravity, and tail fin deflection angle) are fixed at non-zero values [11,12]. The third mode of operation is swimming, and it is achieved by continuously flapping the tail fin to propel the fish forward with steering and velocity being controlled by the bias and amplitude of the flapping [13].

The efficiency of gliding depends on multiple variables, such as pitch angle and maximum depth. Gliding is expected to use less energy when travelling long distances compared to swimming on the surface, as the actuators responsible for adjusting the buoyancy and center of gravity are used in short bursts (10 s-20 s) per glide, while swimming would require continuous flapping of the tail fin. On the other hand, swimming does offer some advatanges over gliding when accurate navigation is needed over a short distance due to the availability of GPS on the surface. Therefore, an efficient navigation strategy needs to leverage gliding and swimming modes effectively when moving from one point to another. The different modes of operation have allowed researchers to use gliding robotic fish for autonomous sampling of harmful algae concentration [4]. During the field experiments, a 60 m-by-80 m region was sampled with a grid of 4-by-5 columns. Figure 2 shows the sampling strategy used in [4]; the robot spirals down a water column while collecting data, and then glides up to the water surface, which generally does not coincide with the next target column. The swimming mode is corrected with GPS-aided guidance, driving the robot to the next column location and repeating the process.

The sampling grid in [4] was predefined and the gathered information was not used to improve future samplings. For better performance, the sampling strategy of the agent should adapt to the information collected during its operation. This process of reactive data gathering is referred to as adaptive sampling, where the agent (the gliding robot fish in this case) changes its path in response to measurements of its own state and the sampled environment [14]. For more information on adaptive sampling, the reader can refer to [14–17].

Adaptive sampling is particularly important for underwater missions, due to the unpredictability of the environment and the limited resources of the agents (e.g. power supply), factors that highlight the need of reactive and efficient sampling. As is discussed in [17], adaptive sampling performance depends on the metric used to evaluate the data sets. For example, prioritizing exploration of areas of high dynamic variability or cluttered locations are two different strategies that can be used with adaptive sampling.

In this paper, we utilize ergodic exploration to generate the sampling trajectory. Ergodic exploration presents a promising framework for dealing with trajectory planning because it aims at regulating the time a robot spends in a region to be propor-

tional to the expected information density [18, 19]. As a result, ergodic trajectories strike a balance between exploration and exploitation strategies. The gliding robotic fish, however, presents a highly nonlinear model with strong coupling of the inputs [20]. To effectively deal with the challenging complexities of finding optimal 3D ergodic trajectories that are feasible for the robot's dynamics, we propose a novel strategy that requires the 2D trajectory optimization, while the robot's energy-efficient spiraling mode is used to sample water columns along the third dimension.

The remainder of this paper is organized as follows: we describe the field of interest in Section II, followed by an overview on the notion of ergodicity in Section III. In Section IV, we present the adaptive sampling strategy of the water columns and in Section V we examine the performance of the proposed strategy in simulation. Finally, concluding remarks and future research directions are provided in Section VI.

Field Representation and Gaussian Regression

The end goal of the sampling strategy is to estimate and reconstruct a three-dimensional field of interest by collecting samples at discrete locations. To that end, we represent the field to be estimated as a Gaussian process (GP) as it provides an elegant method for modeling nonlinear functions in the Bayesian framework [21], and are widely used for modeling spatial fields and spatio-temporal phenomena [22–24]. GP regression has also been widely used to predict the field values at unsampled areas using measurements at discrete locations, and have been extensively used in spatial prediction and reconstruction of a field [21].

We consider a zero-mean Gaussian process $g(p) \in \mathbb{R}$ that is written as

$$g(p) \sim \mathscr{GP}\left(0, \sigma_f^2 \mathscr{K}(p_1, p_2)\right), \tag{1}$$

where $p_1, p_2 \in \mathbb{R}^3$ are the inputs, representing two discrete locations in the 3D space, and $\sigma_f^2 \mathscr{K}(p_1, p_2)$ is the covariance function. The signal variance σ_f^2, which is assumed to be constant across the entire 3D space, gives the overall scale of the field relative to the mean of the GP.

The correlation between $g(p_1)$ and $g(p_2)$ is given by $\mathscr{K}(p_1, p_2)$. In this paper, we use the squared exponential correlation function of the form

$$\mathscr{K}(p_1, p_2) = \exp\left(-\frac{1}{2}(p_1 - p_2)^T \Sigma_l^{-1}(p_1 - p_2)\right). \tag{2}$$

Here, $\Sigma_l = \mathrm{diag}(\sigma_1, \sigma_2, \sigma_3)$ is a diagonal matrix that determines the decreasing rate of the correlation between two points as the distance between them increases along each direction. The parameters $\{\sigma_f, \sigma_1, \sigma_2, \sigma_3\}$ are referred to as the hyperparameters of the GP and can be estimated *a priori* by the maximization of the likelihood function [25]. Here, we assume that the hyperparameters are known *a priori*.

When samples of the field are collected at discrete locations, it is possible to estimate the field values at the remaining unsampled areas through GP regression. Suppose we have r noise-corrupted measurements $\{\psi_1, \ldots, \psi_r\}$ obtained by sampling the field at locations $\{p_1, \ldots, p_r\}$. The measurement noises are assumed to be independent at different locations, and are zero-mean, Gaussian, with σ_w representing the measurement noise variance. Then, the collection of observations $\psi = \begin{bmatrix}\psi_1 & \ldots & \psi_r\end{bmatrix}^T$ has the Gaussian distribution

$$\psi \sim \mathscr{N}\left(0, \sigma_f C\right), \tag{3}$$

where $C \in \mathbb{R}^{r \times r}$ is the correlation matrix of ψ, whose (i, j) element is computed as

$$[C]_{ij} = \mathscr{K}(p_i, p_j) + \frac{\delta_{ij}}{\gamma}. \tag{4}$$

Here, γ is the signal to noise ratio (SNR) defined as $\gamma = \sigma_f^2/\sigma_w^2$, and δ_{ij} denotes the Kronecker delta function. Work in [21] shows that one can predict the value of the Gaussian process at a point $p^\star$ by

$$\hat{g}(p^\star) = q^T C^{-1} \psi \tag{5}$$

with a prediction variance that is given by

$$\sigma^2_{\hat{g}(p^\star)} = \sigma_f^2 (1 - q^T C^{-1} q), \tag{6}$$

where $q \in \mathbb{R}^r$ is the correlation vector between ψ and $g(p^\star)$. The correlation vector is obtained by

$$[q]_j = \mathscr{K}(p_j, p^\star). \tag{7}$$

Using the GP model along with GP regression allows us to estimate the field at unsampled locations. It is still important, however, to select sampling locations that improve this estimation performance. In the next section, we discuss how the notion of ergodicity is used to select such sampling locations.

Ergodic Exploration

When exploring, it is important to prioritize areas with more information. The concept of exploration efficiency is quantified using the measure of ergodicity presented in [19]. A trajectory $x(t)$ is ergodic with respect to some distribution $\phi(x)$

when the percentage of time spent over any subset of the domain is equal to the measure of that subset. Here, the distribution $\phi(x)$ represents the expected information density (EID) map, over a bounded n-dimensional domain $X \subset \mathbb{R}^n$, defined as $[0, L_1] \times [0, L_2] \cdots \times [0, L_n]$. The ergodic metric used to quantify the difference between spatial statistics of $\phi(x)$ and the trajectory $x(t)$ is given by

$$\varepsilon(x(t)) = \sum_{k=0 \in \mathbb{Z}^n}^{K \in \mathbb{Z}^n} \Lambda_k |c_k(x(t)) - \phi_k|^2, \tag{8}$$

where ϕ_k are the Fourier coefficients of the spatial distribution $\phi(x)$, and c_k are the Fourier coefficients of the basis functions along the trajectory $x(t)$ averaged over time. The number of coefficients used along each of the n dimensions to measure distance from ergodicity is determined by K, and k is a multi-index $(k_1, k_2, \ldots, k_n)$. We use Λ_k defined as

$$\Lambda_k = \frac{1}{(1 + \|k\|^2)^s} \tag{9}$$

with $s = \frac{n+1}{2}$ to place larger weight on lower frequency information.

The Fourier coefficients ϕ_k and c_k are computed as follows:

$$\phi_k = \int_X \phi(x) F_k(x) dx \tag{10}$$

and

$$c_k = \frac{1}{T} \int_0^T F_k(x(t)) dt, \tag{11}$$

where $F_k(x)$ are the Fourier basis functions used to approximate the distributions over n dimensions. They are given by

$$F_k(x) = \frac{1}{h_k} \prod_{i=1}^{n} \cos\left(\frac{k\pi}{L_i} x_i\right), \tag{12}$$

where h_k is a normalizing factor and x_i is the i-th component of x. We refer the reader to [18, 19], and references therein for a complete discussion on ergodic exploration.

Adaptive Sampling Strategy

Ergodic exploration presents a promising framework for active exploration as it builds exploration strategies that take into account the dynamics of the sensing agent [18]. This allows us to generate sampling trajectories that are gaurenteed to be feasible, which is in contrast to other adaptive sampling strategies that do not consider robot dynamics and could result in infeasible trajectories [26–28].

The 3D model, described in [20], that involves sophisticated hydrodynamic modeling and strong coupling of the inputs is prohibitive for real-time execution. Moreover, tracking such curves is nontrivial, with limited work reported in that area. To effectively tackle the challenging complexities posed by three-dimensional sampling and exploration of underwater environments, we propose a novel strategy that decomposes the problem into a hybrid problem involving 2D trajectory optimization, with spiraling along the z-direction using the gliding robotic fish for sampling of water columns.

This approach holds several advantages over optimizing a 3D trajectory for underwater sampling. First, the computational effort needed for computing the exploration trajectory is significantly reduced by optimizing the trajectories on a 2D plane, allowing for real time implementation of the exploration strategy. Second, the proposed algorithm ensures that the robot surfaces after each column sample is taken, allowing for accurate localization using the on-board GPS. This is very important when sampling the environment, as exploration stratiegies that spend a long time underwater generally require accurate localization of the robot in a GPS-denied environment, causing the obtained measurements to be unreliable when the uncertainty in the robot's location is high.

For 2D trajectory planning, we propose using a unicycle model traveling at a constant speed v with steering as its only control, whose model is given by

$$\begin{aligned} \dot{p}_x &= v\cos(\theta) \\ \dot{p}_y &= v\sin(\theta) \\ \dot{\theta} &= \omega \end{aligned} \tag{13}$$

Here, (p_x, p_y) represents the unicycle's position on the 2D plane, while θ is its orientation and ω is the steering control. In our previous work in [4], we demonstrated the capability of the robot in autonomously navigating from one point to another. Therefore, the planner motion of the unicyle can be effectively tracked though simple controlled that adjust the tail deflection angle during a glide, or by ajusting the amplitude and bias of the tail flapping when swimming on the surface. Using the unicycle model to plan a 2D trajectory ensures that the robot samples columns sequentially, i.e. the next column to sample is within a predifined distance of the previous column, which in turn ensures that the robot is not travelling between very far points to collect samples. Moreover, the unicycle model results in smooth planar trajectories that minimize sharp turns between two column samples.

The above model is embedded into the ergodic exploration engine to generate optimal 2D trajectories along which the

gliding robotic fish spirals to collect water columns samples. Ergodic-based optimization of the unicycles trajectory requires the use of an appropriate EID quantifying the expected information density for each water column on the 2D plane. This makes GP regression techniques well suited for the ergodic exploration framework as the prediction variance at any point in the field can be computed in closed form using (6).

After each column sample, the measurements obtained by the robot are fed back to the Gaussian process regression model to predict the field at all unsampled locations. In order to steer the unicycle towards informative areas, and therefore select the next sampling location, a 2D EID map must be generated. GP regression allows for the comutation of the prediction variance, $\sigma^2_{\hat{g}(p^\star)}$, in closed form using (6). At first glance, using $\sigma^2_{\hat{g}(p^\star)}$ seems like a good measure of information, as it is equivalent to the notion of entropy of a Gaussian random variable $H(p^\star)$, where more information can be obtained from the locations that are deemed most uncertain. While this provides an intuitive approach, it suffers from two major drawbacks. As noted in [26], the entropy criterion results in "wasted" information, as uncertainty tends to be largest at the boundry of the space. More importantly, using entropy as a measure for placing sensors has been shown to bear no advantages over sampling the space with a uniform grid.

It is important, therefore, to select an appropriate criterion when generating the EID map. One approach is to consider the mutual information between each point and the rest of the space. In [26], the authors present several approximation algorithms for computing mutual information between a point and the rest of the space, which is proportional to

$$MI(p^\star) \propto \frac{\sigma_f^2 - q^T C^{-1} q}{\sigma_f^2 - \bar{q}^T \bar{C}^{-1} \bar{q}}, \tag{14}$$

where $\bar{q}$ is the correlation vector between $p^\star$ and the unsampled points, while $\bar{C}$ is the correlation matrix between all unsampled points. This allows us to generate a 2D EID map for planning the unicycle's trajectory.

We employ a receding-horizon ergodic exploration scheme for planning an exploration trajectory, by tailoring the optimization algorithm to the unicycle model [13, 29]. Using the metric of ergodicity mentioned in the previous section, we define the ergodic objective function to be optimized $J(\cdot)$ as follows

$$J = \sum_{k=0 \in \mathbb{Z}^n}^{K \in \mathbb{Z}^n} \Lambda_k |c_k(x(t)) - \phi_k|^2. \tag{15}$$

This optimization problem can be solved by framing the problem as a hybrid control problem similarly to Sequential Action Control (SAC) in [30]. First, the coefficients ϕ_k of the spatial distribution $\phi(x)$ are calculated, and then the steering control of the unicycle is obtained by solving an open-loop ergodic control problem [29]. The complete strategy for adaptive sampling of water columns using the gliding robotic fish is depicted in Figure 3.

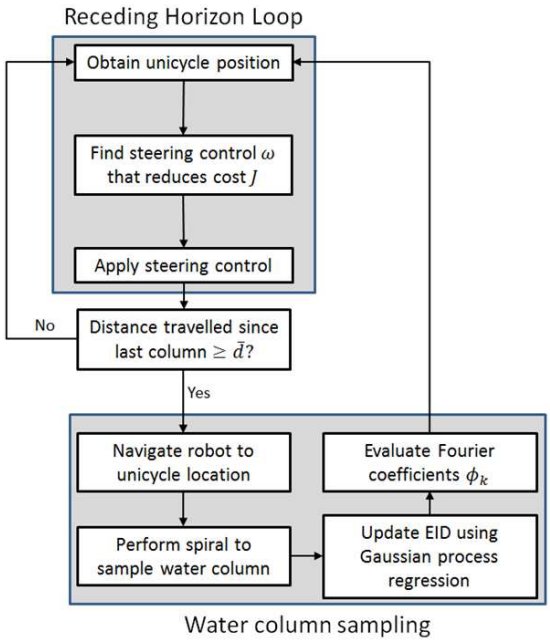

FIGURE 3. Blockdiagram of adaptive strategy for water column sampling. A receding-horizon optimization loop is used to compute the 2D trajectory for the unicycle using the latest available EID. Water columns are sampled along the trajectory, and the collected measurements are used to update the EID through GP regression.

The proposed strategy requires significantly less computational effort when compared to finding an ergodic three-dimensional trajectory that obeys the gliding robotic fish's dynamics, as it only needs to compute a 2D trajectory. Furthermore, the proposed strategy can be adopted to real-world experiments without the need for expensive, and power-hungry, acoustic localization equipment. This is due to the fact that the robot can periodically surface and use GPS measurements to determine its location, while water-pressure and velocity measurements help estimate the position of the agent while underwater.

Simulation Study

We examine the performance of the proposed approach at sampling and reconstructing a region of 80 m-by-80 m, while the depth for each sampled column is set to 7m. The unicycle was initialized at $(x,y) = (5,5)$ and $\theta = 20$, and traveling at a constant speed of 1 m/s. As for the field characterization, the signal variance was set to $\sigma_f = 1$, where $\Sigma_l = \text{diag}(50,50,7)$, and

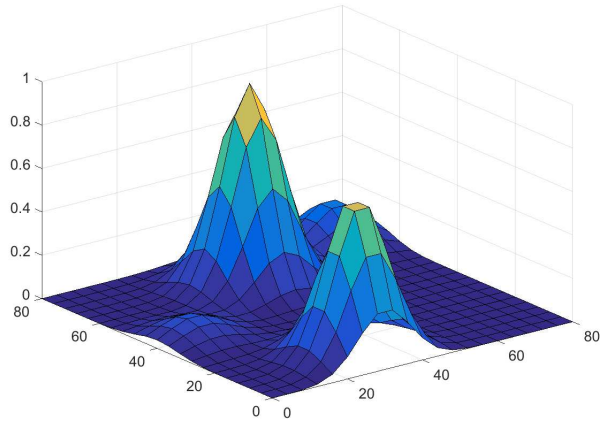

FIGURE 4. Original field at $z = 6$ m.

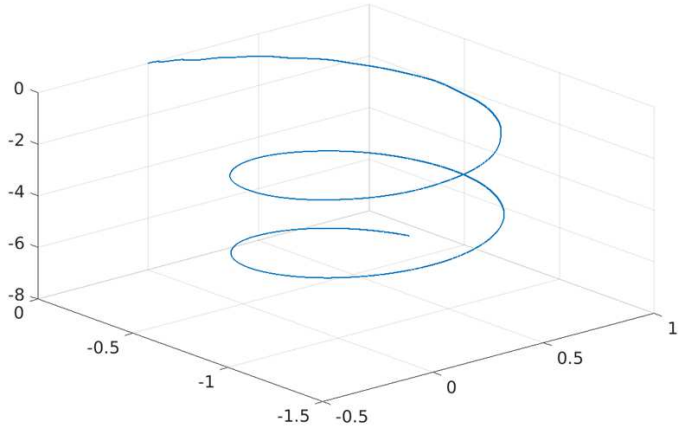

FIGURE 5. Simulated spiral trajectory of gliding robotic fish for fixed control inputs.

the noise standard deviation was set to $\sigma_w = 0.1$. Figure 4 depicts the original field at a depth of $z = 6$ m, which was constructed to have larger values as the depth increases.

Water columns were sampled every 20 m along the optimized trajectory of the unicycle. Figure 5 shows the simulated spiraling trajectory for the gliding robotic fish at each column obtained from using the full 3D model presented in [20], which takes about 3 minutes to complete. Noisy measurements were recorded every 12 s along this spiraling trajectory to be used in the GP regression model.

Figure 6 shows the evolution of the optimized trajectory of the unicycle on the 2D plane along with the locations of the sampled water columns. Initially, the EID is the same everywhere as we have very little information to predict the field, and the prediction error is large everywhere. As the unicycle travels in the 2D plane to reduce the ergodic cost, and column samples are obtained along the way, the prediction error at the sampled locations is reduced, which in turn updates the EID and drives the unicycle away from these sampled locations.

Figure 7 shows the evolution of the field estimates at a depth of $z = 6$ m as more columns are sampled, while Figure 8 depicts the estimation error at different depths after 16 columns were sampled. These figures show the capacity of the proposed approach in reconstructing the original field. Figure 9 compares the estimation error between our proposed approach and that obtained by sampling from a uniform grid of 16 water columns. These results show the advantage of using the proposed approach over uniform sampling, as it forces us to sample more informative areas in the center of the space. In contrast, a uniform grid of 16 columns would have 12 of those columns located on the boundry of the space, resulting in wasted information.

Conclusion and Future Work

In this paper, we propose using ergodic exploration together with adaptive sampling of water columns subject to the dynamics of a gliding robotic fish. To improve the computational speed of our algorithm and to address the challenging complexities of sampling underwater 3D environments, we use the dynamics of a unicycle to model the planar motion, while still using the operational modes of the gliding robotic fish to sample water columns along the trajectory in the remaining dimension. We generate optimized 2D trajectories using the ergodic metric and utilize Gaussian process regression to predict the field values at unsampled locations and to update the EID map that drives ergodic exploration. Future work will focus on the ability of ergodic exploration in estimating the hyper-parameters of the GP, and extending the simulation work to real-world field experiments with our gliding robotic fish.

REFERENCES

[1] Leonard, J. J., and Bahr, A., 2016. "Autonomous underwater vehicle navigation". In *Springer Handbook of Ocean Engineering*. Springer, pp. 341–358.

[2] Murphy, A., Landamore, M., and Birmingham, R., 2008. "The role of autonomous underwater vehicles for marine search and rescue operations". *Underwater Technology,* ***27***(4), pp. 195–205.

[3] Tan, X., 2011. "Autonomous robotic fish as mobile sensor platforms: Challenges and potential solutions". *Marine Technology Society Journal,* ***45***(4), pp. 31–40.

[4] Zhang, F., Ennasr, O., Litchman, E., and Tan, X., 2016. "Autonomous sampling of water columns using gliding robotic fish: Algorithms and harmful-algae-sampling experiments". *IEEE Systems Journal,* ***10***(3), pp. 1271–1281.

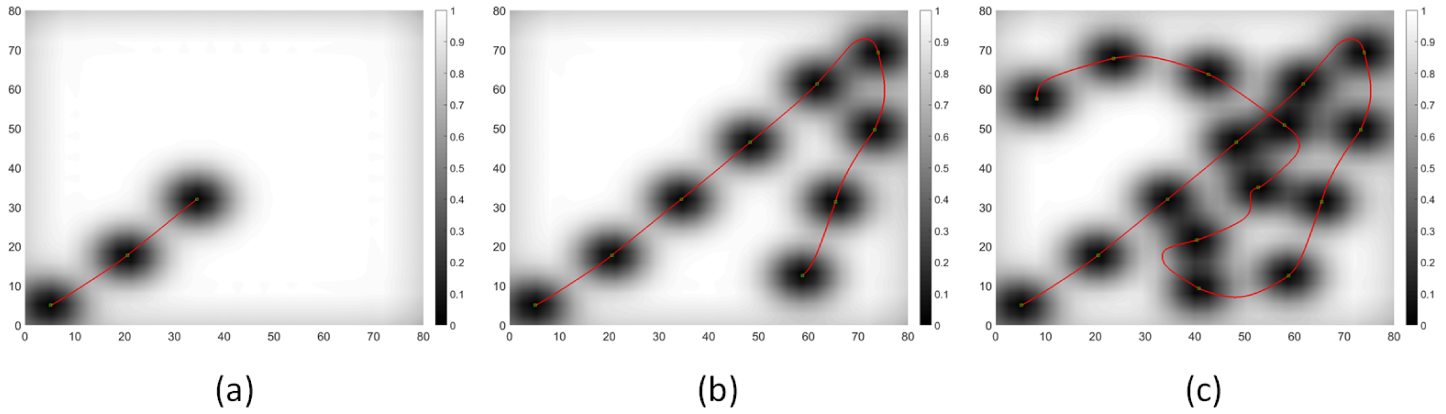

FIGURE 6. Optimized ergodic trajectory of unicycle on the 2D plane (solid red line), along which water column samples are collected (green squares) every 20 m, both overlaying the EID map (grayscale) which reflects the expected information at each location. The three plots show the evolution of the trajectory and EID after (a) 3 columns, (b) 9 columns, and (c) 16 columns have been taken.

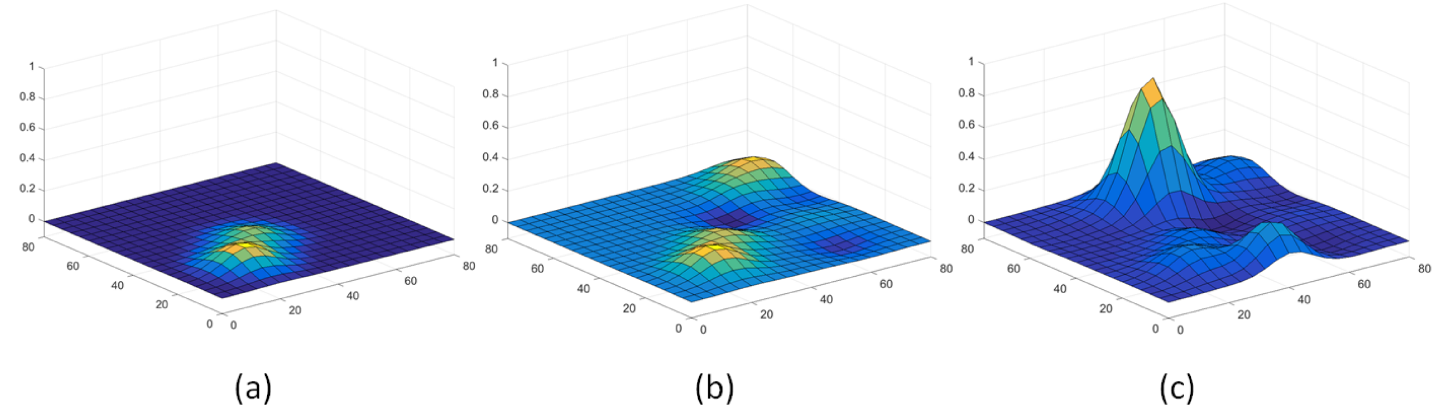

FIGURE 7. Evolution of field estimates at depth $z = 6$ m, after (a) 3 column, (b) 9 columns, and (c) 16 columns have been sampled.

[5] Mitchell, B., Wilkening, E., and Mahmoudian, N., 2013. "Developing an underwater glider for educational purposes". In IEEE International Conference on Robotics and Automation (ICRA), IEEE, pp. 3423–3428.

[6] Sherman, J., Davis, R. E., Owens, W., and Valdes, J., 2001. "The autonomous underwater glider " Spray"". *IEEE Journal of Oceanic Engineering,* ***26***(4), pp. 437–446.

[7] Zhang, F., Thon, J., Thon, C., and Tan, X., 2014. "Miniature underwater glider: Design and experimental results". *IEEE/ASME Transactions on Mechatronics,* ***19***(1), pp. 394–399.

[8] Chen, Z., Shatara, S., and Tan, X., 2010. "Modeling of biomimetic robotic fish propelled by an ionic polymer–metal composite caudal fin". *IEEE/ASME Transactions on Mechatronics,* ***15***(3), pp. 448–459.

[9] Phamduy, P., LeGrand, R., and Porfiri, M., 2015. "Robotic fish: Design and characterization of an interactive idevice-controlled robotic fish for informal science education". *IEEE Robotics & Automation Magazine,* ***22***(1), pp. 86–96.

[10] Zhang, F., Lagor, F. D., Yeo, D., Washington, P., and Paley, D. A., 2015. "Distributed flow sensing for closed-loop speed control of a flexible fish robot". *Bioinspiration & biomimetics,* ***10***(6), p. 065001.

[11] Zhang, S., Yu, J., Zhang, A., and Zhang, F., 2013. "Spiraling motion of underwater gliders: Modeling, analysis, and experimental results". *Ocean Engineering,* ***60***, pp. 1–13.

[12] Zhang, F., Zhang, F., and Tan, X., 2014. "Tail-enabled spiraling maneuver for gliding robotic fish". *Journal of Dynamic Systems, Measurement, and Control,* ***136***(4), p. 041028.

[13] Castaño, M. L., Mavrommati, A., Murphey, T. D., and Tan, X., 2017. "Trajectory planning and tracking of robotic fish using ergodic exploration". In American Control Conference (ACC), pp. 5476–5481.

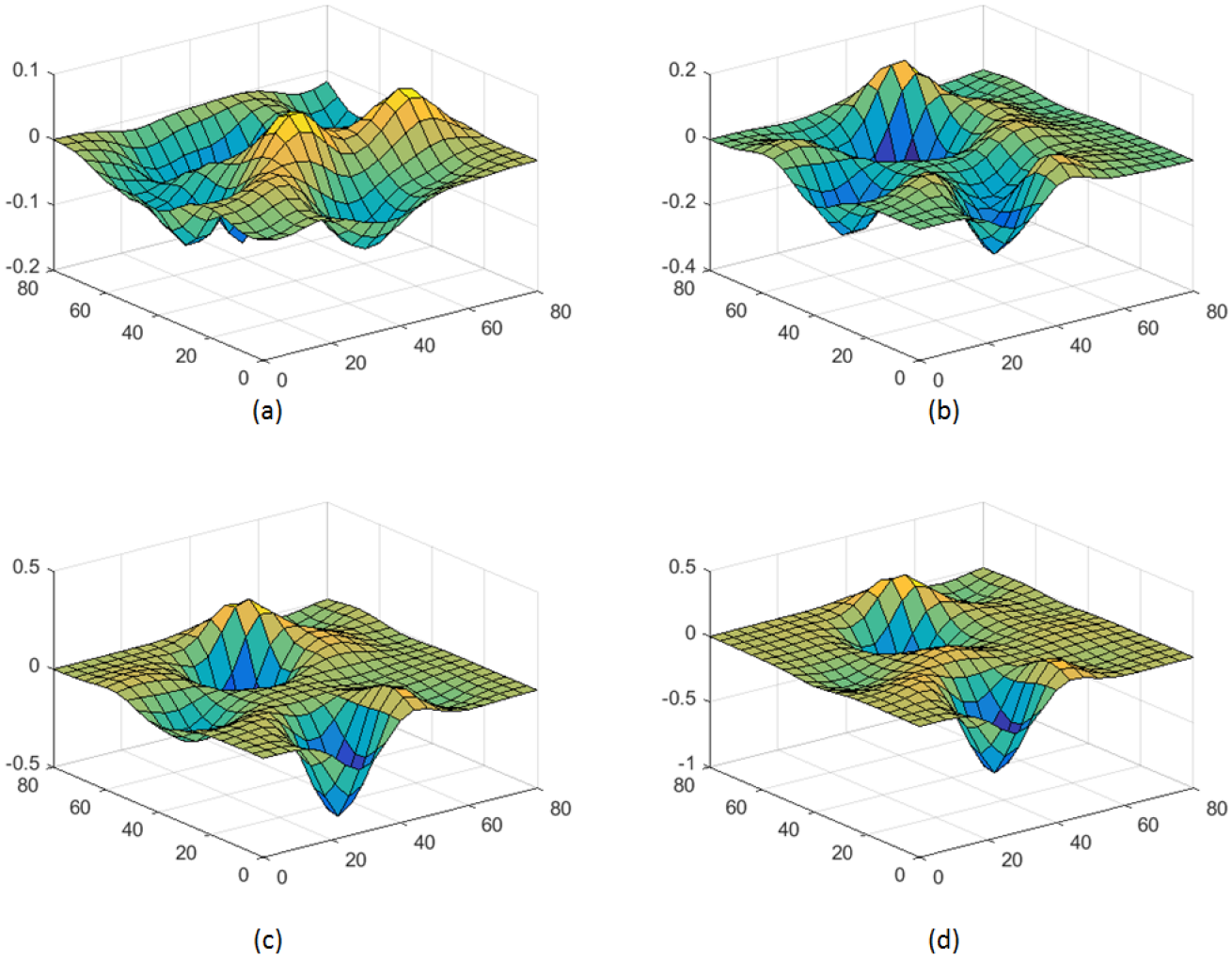

FIGURE 8. Estimation error after 16 columns samples at various depths: (a) $z = 0$ m, (b) $z = 2$ m, (c) $z = 4$ m, and (d) $z = 6$ m.

[14] Leonard, N. E., Paley, D. A., Lekien, F., Sepulchre, R., Fratantoni, D. M., and Davis, R. E., 2007. "Collective motion, sensor networks, and ocean sampling". *Proceedings of the IEEE,* ***95***(1), pp. 48–74.

[15] Fiorelli, E. A., 2005. *Cooperative vehicle control, feature tracking and ocean sampling*. Princeton University.

[16] Fiorelli, E., Bhatta, P., Leonard, N. E., and Shulman, I., 2003. "Adaptive sampling using feedback control of an autonomous underwater glider fleet". In Proceedings of 13th Int. Symp. on Unmanned Untethered Submersible Technology (UUST).

[17] Fiorelli, E., Leonard, N. E., Bhatta, P., Paley, D. A., Bachmayer, R., and Fratantoni, D. M., 2006. "Multi-auv control and adaptive sampling in monterey bay". *IEEE journal of oceanic engineering,* ***31***(4), pp. 935–948.

[18] Miller, L. M., Silverman, Y., MacIver, M. A., and Murphey, T. D., 2016. "Ergodic exploration of distributed information". *IEEE Transactions on Robotics,* ***32***(1), pp. 36–52.

[19] Mathew, G., and Mezić, I., 2011. "Metrics for ergodicity and design of ergodic dynamics for multi-agent systems". *Physica D: Nonlinear Phenomena,* ***240***(4), pp. 432–442.

[20] Zhang, F., 2014. "Modeling, design and control of gliding robotic fish". PhD thesis, Michigan State University.

[21] Rasmussen, C. E., and Williams, C. K., 2006. *Gaussian Processes for Machine Learning*, Vol. 1. MIT press Cambridge.

[22] Andugula, P., Durbha, S. S., Lokhande, A., and Suradhaniwar, S., 2017. "Gaussian process based spatial modeling of soil moisture for dense soil moisture sensing network". In International Conference on Agro-Geoinformatics, pp. 1–5.

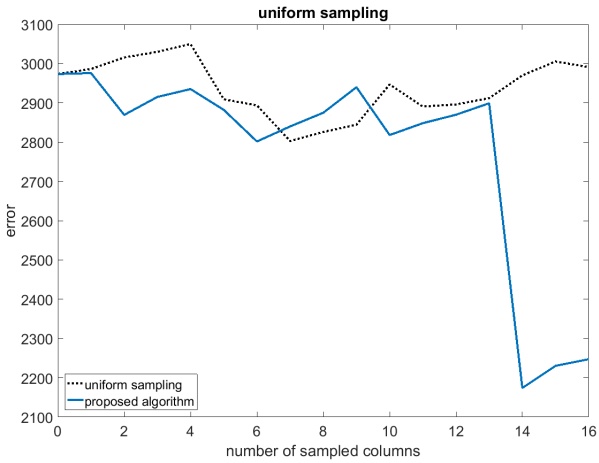

FIGURE 9. Comparison of estimation error, integrated over the entire space, between the proposed algorithm and a uniform grid of 16 columns.

[23] Stamenkovic, J., Guerriero, L., Ferrazzoli, P., Notarnicola, C., Greifeneder, F., and Thiran, J. P., 2017. "Soil moisture estimation by sar in alpine fields using gaussian process regressor trained by model simulations". *IEEE Transactions on Geoscience and Remote Sensing,* ***55***(9), Sept, pp. 4899–4912.

[24] Nguyen, L. V., Kodagoda, S., Ranasinghe, R., Dissanayake, G., Bustamante, H., Vitanage, D., and Nguyen, T., 2014. "Spatial prediction of hydrogen sulfide in sewers with a modified gaussian process combined mutual information". In International Conference on Control Automation Robotics Vision (ICARCV), pp. 1130–1135.

[25] Xu, Y., Choi, J., and Oh, S., 2011. "Mobile sensor network navigation using gaussian processes with truncated observations". *IEEE Transactions on Robotics,* ***27***(6), pp. 1118–1131.

[26] Krause, A., Singh, A., and Guestrin, C., 2008. "Near-optimal sensor placements in gaussian processes: Theory, efficient algorithms and empirical studies". *Journal of Machine Learning Research,* ***9***(Feb), pp. 235–284.

[27] Huang, S., and Tan, J., 2012. "Adaptive sampling using mobile sensor networks". In 2012 IEEE International Conference on Robotics and Automation, pp. 657–662.

[28] Jnsson, P. B., Wang, J., and Kim, J., 2017. "Scalar field reconstruction based on the gaussian process and adaptive sampling". In 2017 14th International Conference on Ubiquitous Robots and Ambient Intelligence (URAI), pp. 442–445.

[29] Mavrommati, A., Tzorakoleftherakis, E., Abraham, I., and Murphey, T. D., 2017. "Real-time area coverage and target localization using receding-horizon ergodic exploration". *arXiv preprint arXiv:1708.08416*.

[30] Ansari, A. R., and Murphey, T. D., 2016. "Sequential action control: Closed-form optimal control for nonlinear and nonsmooth systems". *IEEE Transactions on Robotics,* ***32***(5), pp. 1196–1214.